Risk Management and Healthcare Policy

Dovepress
Taylor & Francis Group

Open Access Full Text Article

ORIGINAL RESEARCH

Development and Validation of a Diagnostic Nomogram for Pathologic Myopia in Patients with High Myopia and Tessellated Fundus: A Cross-Sectional Study

Huiyi Zuo[1,*], Hai Huang[2,*], Baoyu Huang[1], Jian He[1], Xin Liu[1], Haohui Zhou[3], Lijia Huang[1], Fulan Bi[1], Minli Huang[1,*]

[1]Department of Ophthalmology, The First Affiliated Hospital of Guangxi Medical University, Nanning, Guangxi Zhuang Autonomous Region, 530000, People's Republic of China; [2]Department of Ophthalmology, Beiliu City People's Hospital, Beiliu, Guangxi Zhuang Autonomous Region, 537400, People's Republic of China; [3]School of Medical Technology and Engineering, Fujian Medical University, Fuzhou, Fujian Province, 350000, People's Republic of China

*These authors contributed equally to this work

Correspondence: Minli Huang, Department of Ophthalmology, The First Affiliated Hospital of Guangxi Medical University, No. 6, Shuangyong Road, Nanning, Guangxi Zhuang Autonomous Region, 530000, People's Republic of China, Tel +86-771-5356507, Email 420306@sr.gxmu.edu.cn

Purpose: Early identification of pathological changes in high myopia (HM) with tessellated fundus (TF) remains challenging. To address this, a diagnostic nomogram was developed and validated to aid clinical screening of pathologic myopia (PM) in HM patients with TF.

Patients and Methods: A cross-sectional study was performed at The First Affiliated Hospital of Guangxi Medical University between May 10, 2023, and March 31, 2024. Patients with HM, defined as a spherical refractive error of ≤ −6.0 D or an axial length of ≥ 26.5 mm, who presented with TF were enrolled. The collected clinical data were randomly divided into training and validation sets at a 7:3 ratio. A diagnostic nomogram was constructed from independent predictive factors. Its discrimination, calibration, and clinical utility were assessed using receiver operating characteristic (ROC) curves, calibration curves, and decision curve analysis (DCA).

Results: Data from 418 eyes with TF were included in this study. Independent predictors for PM, in descending order of association, were axial length, optic disc tilt ratio, spherical equivalent, education level, and extent of peripapillary atrophy. The nomogram demonstrated robust performance in both sets. In the training set, the area under the ROC curve (AUC) was 0.851 (95% CI: 0.808–0.895), with a sensitivity of 0.775 and a specificity of 0.736. In the validation set, the AUC was 0.827 (95% CI: 0.755–0.900), with a sensitivity of 0.773 and a specificity of 0.700.

Conclusion: This simple predictive model, developed and validated using common interpretable clinical and fundus imaging features, serves as a valuable tool for screening PM in HM patients with TF.

Keywords: high myopia, pathologic myopia, nomogram, tessellated fundus, interpretable model

Introduction

Myopia is widely recognized as a major public health issue that leads to substantial vision loss and is a risk factor for various other serious ocular diseases. In 2000, there were 1.406 billion individuals with myopia (22.9% of the world population) and 163 million individuals with high myopia (HM; 2.7% of the world population) worldwide. It is estimated that there will be 4.758 billion individuals with myopia (49.8% of the world population) and 938 million individuals with HM (9.8% of the world population) by 2050.[1] As HM progresses, the axial length elongates and mechanically stretches the eye wall, leading to various pathological changes in the myopic fundus such as posterior scleral staphyloma, chorioretinal atrophy, lacquer crack formation, and neovascularization. These changes ultimately result in loss of best corrected visual acuity (BCVA).[2] In adults over 40, the incidence of pathologic myopia (PM) is approximately 1% in

Received: 24 June 2025
Accepted: 24 October 2025
Published: 1 November 2025

Caucasian populations and 1–3% in Asian populations.[3] PM has become a major cause of visual impairment, accounting for 12–27% of low-vision cases in China and Japan.[4]

According to the International Photographic Classification and Grading System (META-PM),[5] the newly developed ATN classification system based on the three major myopic changes-atrophy (A), traction (T) and neovascularization (N)[6]-and previous studies,[7,8] a tessellated fundus (TF) is defined as the increased visibility of large choroidal vessels at the posterior fundus pole, which is an early manifestation of myopic atrophic maculopathy (category 1). In HM patients with PM, axial length elongation and eyeball stretching lead to ocular wall thinning, degeneration of choroidal vessels, and progressive thinning and atrophy of the retinal pigment epithelium (RPE). Some TF changes can progress to diffuse atrophy and macular atrophy, resulting in severe and irreversible visual impairment.[9] In addition to myopic atrophic maculopathy, other posterior changes in PM include myopic traction and neovascular maculopathy, posterior scleral staphyloma, and myopia-related glaucomatous optic neuropathy (GON). These pathological changes also occur in patients with TF and are often missed clinically.

Early and accurate identification of pathological fundal changes in HM patients remains challenging in hospitals with limited medical resources, insufficient ophthalmologists, and inadequate access to advanced medical equipment. In China, these limitations often stem from the uneven distribution of medical facilities between urban and rural areas, which affects the coverage and accessibility of fundus screening. Although fundus photography, optical coherence tomography (OCT), fundus autofluorescence imaging, and artificial intelligence-assisted image analysis are currently available for early pathologic myopia (PM) diagnosis,[4] their widespread application remains challenging in resource-limited settings. Therefore, developing a practical screening tool for early and simple PM identification in TF patients under limited ophthalmic resources is an urgent priority. In the present study, we collected interpretable clinical features and fundus imaging features to identify independent predictors of PM. Based on these predictors, a diagnostic nomogram was constructed to provide a practical tool for the early detection of pathological lesions in HM patients with TF.

Materials and Methods

Populations

Clinical data were collected in a cross-sectional study from HM patients diagnosed with TF (defined as increased visibility of large choroidal vessels at the posterior fundal pole[8]) at The First Affiliated Hospital of Guangxi Medical University from May 10, 2023, to March 31, 2024. The inclusion criteria for this study were: (1) Subjects with grade ≥ 1 TF were enrolled to ensure that the study population had discernible choroidal changes. Grading was performed based on the visibility of choroidal vessels using a previously reported classification system.[10] Fundus image quality, including contrast, brightness, and background pigmentation, was assessed through comparison with standard reference images to ensure subjective evaluation. Grading was conducted independently by two ophthalmologists (Huang and He) with over 10 years of experience in retinal disorders. Discrepancies were resolved through discussion and consensus. Two independent batches of fundus images were randomly sampled and evaluated in a blinded study, with the re-evaluation completed two weeks after the first. The inter-observer agreement, as measured by the kappa statistic, exceeded 0.8; (2) Myopia $\leq$-6.0D (excluding cylinder) or axial length $\geq$ 26.5mm; (3) Not received intervention for controlling myopia. Exclusion criteria: (1) Secondary myopia, such as retinopathy of prematurity, history of neonatal disease, or known genetic disorder or connective tissue disorder, such as Marfan syndrome; (2) History of refractive surgery (including corneal refractive surgery, intraocular refractive surgery, and posterior scleral reinforcement) or any intraocular surgery affecting refractive status; (3) Retinal vascular disease, inflammatory diseases of the retina and choroid, tumors of the retina and choroid, congenital choroidal diseases; (4) Autoimmune disorders, such as systemic lupus erythematosus and rheumatoid arthritis; (5) Severe systemic disease such as end-stage heart disease, nephropathy, pulmonary disease, or advanced cancer; (6) Patient with refractive media opacity affecting fundus examination (dense corneal opacity, lens opacity or vitreous opacity). This study was conducted in accordance with the principles of the Declaration of Helsinki and was approved by the Institutional Review Board of The First Affiliated Hospital of Guangxi Medical University (Ethics Approval No.2023-K117-01). All participants or guardians of participants under the age of 18 have signed the informed consent form.

Covariates

Demographic characteristics, visual habits, and family history of myopia were collected from all participants using a standardized questionnaire. Demographics of the subjects included sex, age, height, weight, education level, and age of myopia onset. Eye habits included the daily duration and pattern of eyeglass wear, daily time spent using electronic devices (cellphone, iPad, and computer), the distance at which the cellphone was held from the eyes, daily duration of reading and writing, the distance between the eyes and reading/writing materials, daily duration of outdoor activities, and the type of lighting used. Family history of myopia mainly included parental myopia (presence or absence of myopia in either parent) and myopia in the family. Ocular parameters were measured using standard ophthalmic instruments, including visual acuity, cycloplegic refraction, wide-field scanning laser fundus imaging (Clarus 500, Carl Zeiss Meditec AG, Jena, Germany), optical biometry (IOL-Master 500, Carl Zeiss Meditec AG, Jena, Germany), and corneal topography (Pentacam, Oculus Optikgeräte GmbH, Wetzlar, Germany). Spherical equivalent was calculated as the spherical power plus half of the cylindrical power. All values were expressed as negative for myopic refractive error. The optical biometry included axial length, anterior chamber depth, white-to-white distance, pupil diameter, and keratometry. The corneal topography included corneal thickness, anterior chamber depth, anterior chamber volume, lens thickness, and keratometry. The optic disc area, peripapillary atrophy (PPA; characterized by an inner crescent-shaped area of retinal and choroidal atrophy, with visible large choroidal vessels and sclera[11]), maximum width of PPA, extent of PPA (angular extent of PPA measured from the center of the optic disc. The PPA angle is classified as > 180° if the circumferential span of PPA exceeded 180°), horizontal diameter of the optic disc, vertical diameter of the optic disc, shortest diameter of the optic disc, longest diameter of the optic disc, distance from macula to papilla, optic disc tilt ratio (optic disc tilt is defined by optic disc tilt index, ie shortest diameter to longest diameter ratio of optic disc ≤ 0.8 is defined as optic disc tilt[12]), and optic disc rotation angle (the degree of deviation of the long axis of the optic disc from the vertical line of the horizontal line connecting the macular fovea to the center of the optic disc[13]) were measured using the supporting software of an ultra-widefield fundus imaging system. Specifically, PPA and other optic disc parameters were manually measured from the fundus photographs of each patient by two trained evaluators (Huang and Bi). The consistency of measurements between the two observers was assessed using the intraclass correlation coefficient (ICC) to ensure data reliability (mean ICC = 0.955).

PM Diagnosis

PM is caused by excessive axial elongation associated with myopia, leading to structural changes in the posterior pole of the eye (including posterior scleral staphyloma, myopic maculopathy, and HM-related optic neuropathy) and consequently the loss of BCVA.[2] Myopia-related GON was assessed using visual field testing (Humphrey Field Analyzer 3, Carl Zeiss Meditec AG, Jena, Germany) and optic disc OCT examination (Heidelberg Spectralis OCT, Heidelberg Engineering GmbH, Heidelberg, Germany). Presence of posterior scleral staphyloma and retinal detachment was detected by B-scan ultrasound (Aviso B-scan ultrasound system, Quantel Medical, D'auvergne Cedex, France). Retinal tractional maculopathy and neovascular maculopathy were evaluated in macular OCT examination. Subjects with TF who exhibited retinal schisis, retinal detachment, macular hole, myopic choroidal neovascularization, Fuchs' spots, lacquer cracks, or posterior scleral staphyloma were classified as having PM.[2,5,8,14] Classification and grading of myopic maculopathy, posterior uveal changes, and HM-associated optic neuropathy were independently performed by two trained evaluators (Zuo and Liu) who were blinded to the subjects' demographic, refractive, and ocular biometric data. The inter-observer weighted kappa (95% confidence interval) exceeded 0.8, indicating good agreement.

Sample Size Estimation

Assuming approximately 10 independent predictors for PM and an events-per-variable (EPV) ratio greater than 15, a minimum of 150 PM cases were initially required for the training set. To estimate the total number of cases needed, we referred to Chen et al, who reported that the prevalence of myopic maculopathy between 2016 and 2018 was 66.5% among ≥ 50-year-old HM patients in urban and rural areas of Shanghai.[12] Based on this prevalence, 226 cases were estimated to be required for the training set. Considering a ratio of 7:3 between the training set and the validation set, 96 cases were estimated for the validation set, resulting in a total sample size of 322 HM patients.

Imputation of Missing Values

In our dataset, the variables age at myopia onset, timing of eyeglass replacement, daily duration of eyeglass wear, pattern of eyeglass use, daily sleep duration, daily duration of reading while lying down, axial length, anterior chamber depth, white-to-white distance, pupil diameter, lens thickness, horizontal diameter of the optic disc, vertical diameter of the optic disc, shortest diameter of the optic disc, longest diameter of the optic disc, and optic disc tilt ratio had missing values, with the highest missing rate reaching 4%. Multiple imputation was used to address these missing data.

Model Construction and Validation

The collected data were divided into a training set and a validation set at a 7:3 ratio. Specifically, a random seed of 20180126 was set. For each case, a random number uniformly distributed between 0 and 1 was generated. The data were then sorted according to these random numbers. The lower 70% of the data were assigned to the training set, while the upper 30% were assigned to the validation set. In the training set, variables with $P<0.1$ in the univariate analysis were included in the multivariate stepwise regression to identify independent predictors. A diagnostic nomogram was then constructed based on these independent predictors using logistic regression. The accuracy, calibration, and clinical utility of the nomogram for the training and validation sets were evaluated using the receiver operating characteristic (ROC) curve, calibration curve, and decision curve analysis (DCA).

To account for potential age-related confounding, a stratified analysis was conducted for patients younger than 18 years and those aged 18 years or older.

To verify the robustness of the model, sensitivity analyses were performed. The dataset was further divided at ratios of 8:2, 6:4, and 5:5, and diagnostic nomograms were reconstructed on each subset to assess their accuracy and calibration under different splitting ratios.

Statistical Analysis

Statistical analyses were performed using R 4.5.1. The packages used for model construction included glmnet, pROC, mice, readxl, rmda, and rms. Continuous variables were described according to their distribution. Normally distributed variables were presented as mean ± standard deviation and compared using independent-sample *t*-tests. Skewed variables were presented as median (interquartile range) and compared using the Mann–Whitney *U*-test. Categorical variables were expressed as percentages and compared using the χ^2 or Fisher's exact test. All tests were two-sided, and a P value < 0.05 was considered statistically significant.

Results

General Patient Characteristics

A final total of 418 eyes (118 male eyes and 300 female eyes) were included in this study. The mean age of participants was 27.49 ± 9.78 years, and the majority had attained undergraduate or postgraduate education. A total of 262 eyes had PM, while 156 eyes were classified as non-PM. Of all included eyes, 293 eyes were assigned to the training set and 125 to the validation set. Within the training set, 187 eyes were diagnosed with PM (Table S1).

Analysis of Independent Predictors

Univariate analysis showed that several factors had significant associations with PM. Variables with P values <0.05 included age, BMI, educational level, diopter, daily sleep duration, head tilt, daily duration of reading while lying down, spherical equivalent, axial length, keratometry, anterior chamber volume, PPA area, maximum PPA width, extent of PPA, and optic disc tilt ratio. These findings suggested that they may be independent predictors of PM. In contrast, no significant associations were found for pattern of eyeglass use, daily duration of outdoor activities, corneal thickness, lens thickness, shortest disc diameter, distance from macula to papilla, and optic disc tilt ($0.05 < P < 0.1$). Based on these results, variables with $P < 0.1$ were incorporated into the multivariate stepwise regression (Table S2).

Multivariate stepwise regression showed that independent predictors for PM in HM patients with TF, in descending order of association, were axial length, optic disc tilt ratio, spherical equivalent, education level, and extent of PPA (Table 1).

Table 1 Multivariate Stepwise Regression

Variable	B	SE	χ^2	*P*	OR	95% CI of OR	
						Lower Limit	Upper Limit
Education level (Middle school (ref))			22.050	<0.001			
Bachelor	1.487	0.449	10.979	<0.001	4.424	1.836	10.662
Master	2.799	0.597	22.011	<0.001	16.422	5.101	52.869
Spherical equivalent	0.243	0.101	5.821	0.016	1.274	1.047	1.552
Axial length	1.247	0.201	38.700	<0.001	3.481	2.350	5.157
Extent of PPA (≤180°(ref))							
Extent of PPA (>180°)	1.077	0.454	5.613	0.018	2.935	1.204	7.152
Optic disc tilt ratio	−6.227	1.630	14.601	<0.001	0.002	0.001	0.048
Constant	−31.769	5.384	34.822	<0.001			

Construction of a Nomogram

A nomogram was constructed based on these independent predictors for the diagnosis of pathological changes in HM with TF. For education, middle school served as the reference category, with 14.9 assigned for a bachelor's degree and 28.1 for a master's degree. For spherical equivalent, each 1D increase in the negative value corresponded to a 2.44-point increase in score. For axial length, each 1 mm increase corresponded to a 12.5-point increase. For the extent of PPA ≤180° was used as the reference, with >180° assigned 10.8. For optic disc tilt ratio, a decrease of 0.1 corresponded to a 5.63-point increase in score. The nomogram showed excellent performance in the training set. The ROC curve yielded an area under the ROC curve (AUC) of 0.851 (95% CI: 0.808–0.895). At a threshold probability of 0.587, sensitivity was 0.775, and specificity was 0.736, both of which were the highest. The bootstrap calibration curve demonstrated strong agreement between predicted and observed outcomes. DCA further confirmed that the model provided net benefit across a wide range of threshold probabilities (Figures 1A–D).

Model Validation

In the validation set, the nomogram maintained strong performance with an AUC of 0.827 (95% CI: 0.755–0.900). At the same threshold probability (0.587), sensitivity and specificity were 0.773 and 0.700. Both the calibration curve and DCA indicated favorable calibration and consistent net benefit (Figure 2A–C).

Stratified analysis was conducted to evaluate diagnostic performance across age groups. The AUC was 0.889 (95% CI: 0.715–1.000) in patients <18 years, and 0.821 (95% CI: 0.742–0.901) in those ≥18 years. These results demonstrate that the model retains robust diagnostic value across different age groups (Figure 3A and B).

Sensitivity Analysis

Based on the above independent predictors, the dataset was further divided into training and validation cohorts at ratios of 8:2, 6:4, and 5:5 to construct diagnostic nomograms. At the 8:2 ratio, the training set achieved an AUC of 0.863 (95% CI: 0.824–0.901) with a threshold probability of 0.611, corresponding to a sensitivity of 0.767 and a specificity of 0.774 (Figure S1). The validation set yielded an AUC of 0.776 (95% CI: 0.676–0.875), with a sensitivity of 0.769 and a specificity of 0.625 at the same threshold (Figure S2). At the 6:4 ratio, the training set showed an AUC of 0.846 (95% CI: 0.798–0.895) with a threshold probability of 0.407, corresponding to a sensitivity of 0.951 and a specificity of 0.562 (Figure S3). The validation set achieved an AUC of 0.842 (95% CI: 0.783–0.901), with a sensitivity of 0.870 and a specificity of 0.552 at the same threshold (Figure S4). At the 5:5 ratio, the training set yielded an AUC of 0.841 (95% CI: 0.787–0.895) with a threshold probability of 0.458, corresponding to a sensitivity of 0.904 and a specificity of 0.608

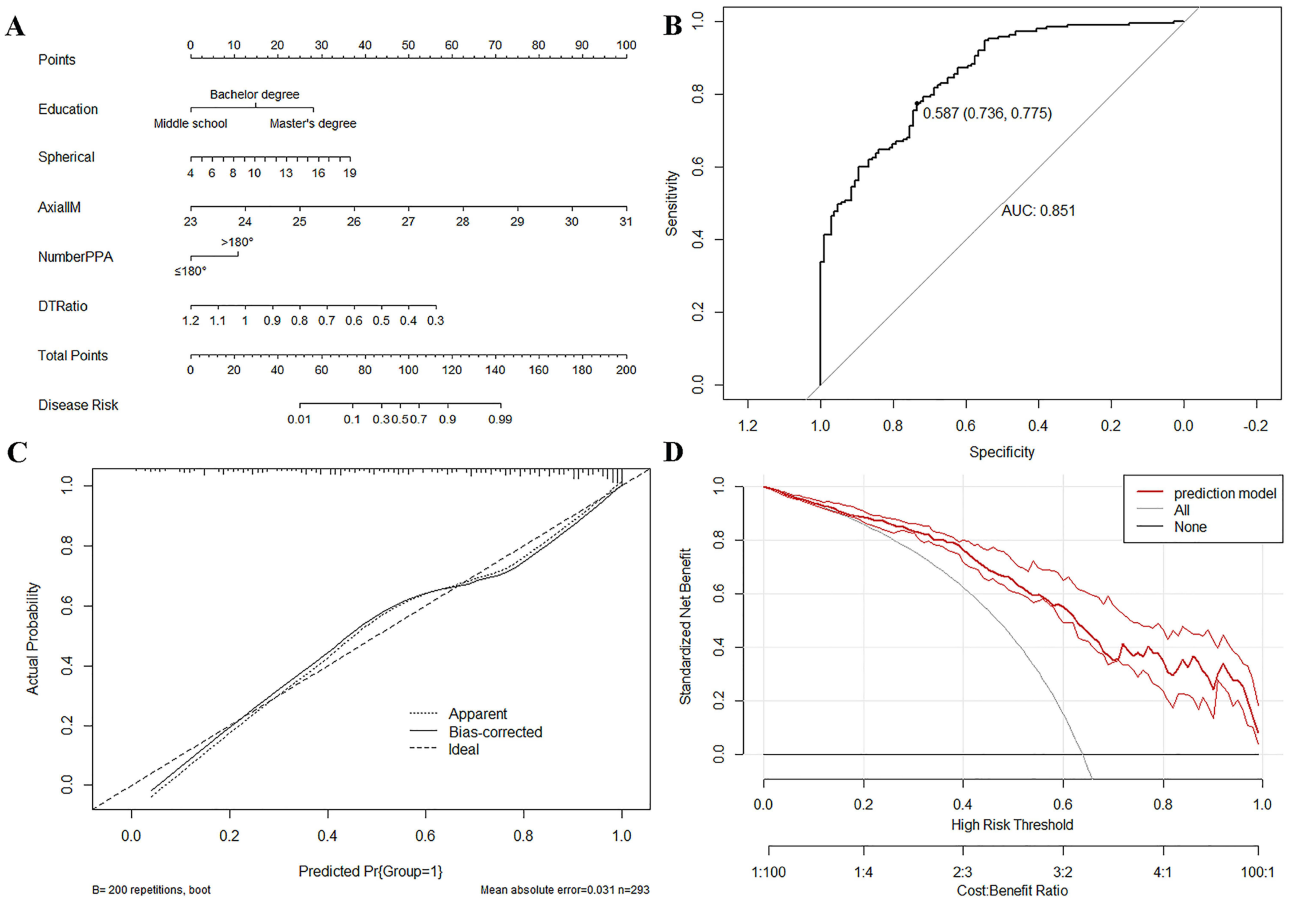

Figure 1 (**A**) Diagnostic nomogram for predicting pathologic myopia in patients with tessellated fundus (Note: Education - education level; Spherical - spherical equivalent (-D); AxialIM - axial length (mm); NumberPPA - extent of peripapillary atrophy; DTRatio - optic disc tilt ratio.); (**B**) Receiver operating characteristic curve (ROC) of nomogram for predicting pathologic myopia in the training set; (**C**) Calibration curve of nomogram for predicting pathologic myopia in the training set; (**D**) Decision curve analysis (DCA) of nomogram for predicting pathologic myopia in the training set.

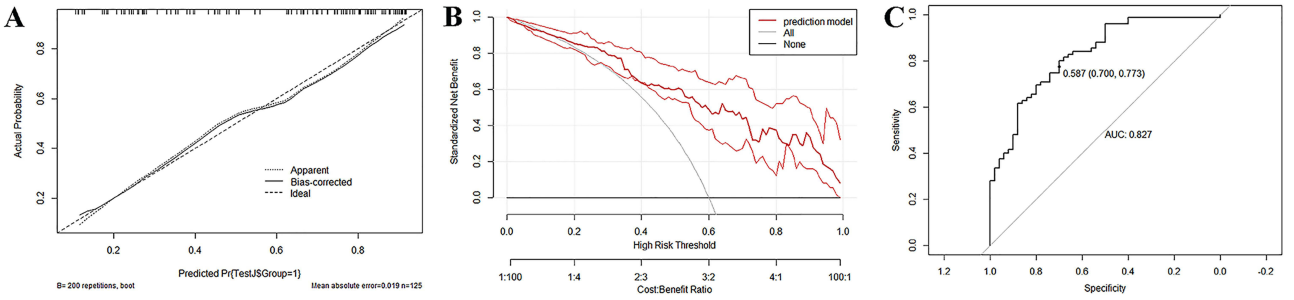

Figure 2 (**A**) Receiver operating characteristic curve (ROC) of nomogram for predicting pathologic myopia in the validation set; (**B**) Calibration curve of nomogram for predicting pathologic myopia in the validation set; (**C**) Decision curve analysis (DCA) of nomogram for predicting pathologic myopia in the validation set.

(Figure S5). The validation set achieved an AUC of 0.847 (95% CI: 0.795–0.899), with a sensitivity of 0.874 and a specificity of 0.610 at the same threshold (Figure S6). Across all dataset partition ratios, the constructed models demonstrated good calibration and high clinical applicability.

Discussion

Our study demonstrated that education level, spherical equivalent, axial length, extent of PPA, and optic disc tilt ratio are independent predictors for pathological changes in HM patients with TF. The resulting interpretable nomogram showed

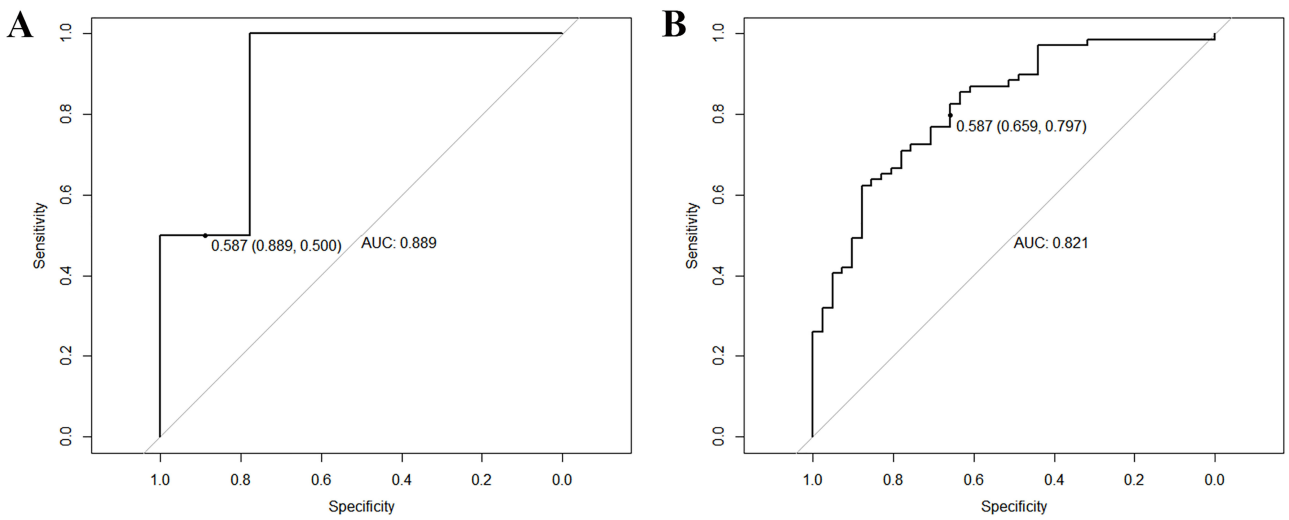

Figure 3 (**A**) Receiver operating characteristic (ROC) curve for the <18 years group; (**B**) Receiver operating characteristic (ROC) curve for the ≥18 years group.

good discrimination in the validation set (AUC = 0.827; 95% CI, 0.755–0.900), with sensitivity of 0.773 and specificity of 0.700. Moreover, under different random split ratios, the constructed models all exhibited satisfactory discrimination in the validation cohorts.

Prior work has highlighted the diagnostic value of image-based machine learning (ML) and deep learning (DL) for PM, especially using fundus or OCT images. ML-based approaches for analyzing the optic disc area during clinical examination can identify less readily detectable myopic maculopathy.[4] While DL often achieves excellent accuracy, performance, and outputs vary across studies, limiting generalizability and interpretability. A meta-analysis of 11 fundus image-based DL studies reported a pooled SROC of 0.9905, specificity of 0.959 (95% CI: 0.955–0.962), and sensitivity of 0.965 (95% CI: 0.963–0.966), but did not evaluate conventional (non-DL) ML models.[15] These findings underscore the need for diagnostic tools that balance performance with stability and transparency.

On the other hand, several research groups have attempted to establish diagnostic models for PM based on interpretable clinical characteristics and lifestyle factors. For instance, Kim et al[16] developed a model incorporating posterior scleral morphology, axial length, and choroidal thickness in HM patients, which achieved an AUC of 0.868, with a sensitivity of 0.800 and specificity of 0.936. Liu et al[17] reported a model based on PPA and clinical image features with an accuracy of 0.875, sensitivity of 0.850, and specificity of 0.900. However, their cohorts mainly included general HM populations without fundus-based classification, which may explain the higher apparent performance.

Focusing on HM eyes with TF, an early and often atypical stage that complicates diagnosis, we developed a logistic-regression nomogram integrating clinical features and lifestyle variables. Although its AUC was lower than that reported by Kim et al and Liu et al, its population specificity improves clinical relevance for targeted subgroups. Logistic regression was deliberately chosen for its transparency and ease of clinical application, offering interpretable estimates of variable contributions compared with the “black box” nature of DL models. This traditional approach also enhanced robustness and generalizability. Future studies may evaluate advanced ML methods to further improve predictive accuracy while maintaining interpretability.

Education level, spherical equivalent, axial length, extent of PPA, and optic disc tilt ratio were independent predictors for PM in HM with TF. Among the independent predictors, axial length and optic disc tilt ratio showed the strongest associations with PM. In the risk scoring system, each 1-mm increase in axial length corresponded to a 12.5-point increase, highlighting its dominant role in disease progression. Similarly, every 0.1 decrease in disc tilt ratio was associated with a 5.63-point increase, indicating that optic disc tilt is another major contributor. Progressive axial elongation alters globe geometry and predisposes to posterior scleral staphyloma, particularly around the disc and macula. Optic disc tilt, defined by a tilt ratio (shortest/longest disc diameter) ≤ 0.8,[12] reflects oblique optic nerve insertion and is common in myopic eyes; greater tilt has been linked to longer axial length,[18,19] worse visual-field

sensitivity, and macular complications.[20] PPA involvement also correlated with PM risk. Compared with ≤180°, involvement exceeding 180° corresponded to a 10.8-point increase in risk score. Larger PPA areas are associated with disc tilt[21,22] and may precede staphyloma and lacquer cracks, eventually contributing to retinal and choroidal atrophy.[23,24] Wang et al characterized the anatomical changes in participants with myopia and glaucoma, identifying PPA expansion as a hallmark of PM, with involvement exceeding 180° suggesting pathological progression.[25] The development or enlargement of PPA is a risk factor for the progression of myopic maculopathy and for progression from HM to PM.[26,27] These anatomical changes provide a plausible pathway from HM to pathological remodeling.

Sociodemographic factors, education level, or lifestyle may also play a role in the progression of HM to PM.[28–31] In the present study, multivariable analysis showed that, beyond ocular characteristics, educational level was the only independent predictor. Compared with middle school education, patients with a bachelor's or master's degree had risk scores of 14.9 and 28.1, indicating a relatively higher PM risk among those with higher education. This finding partially aligns with previous reports. For example, Baird[32] reported a significant association between educational attainment and HM risk. Tedja[33] found in large cohorts from Singapore and Europe that higher educational levels amplified the pathogenic effects of genetic variants such as DNAH9, GJD2, and ZMAT4, and that the combination of high genetic load and university education markedly increased the risk of myopia compared with either factor alone. It is hypothesized that higher educational attainment increases near-work exposure. This may magnify the influence of genetic risk on refractive status, thereby accelerating myopia progression and increasing the likelihood of HM and PM. Therefore, the present findings partially supplement and validate existing evidence, suggesting that educational level should be considered in PM prevention and intervention across populations. Notably, in this study, no significant associations were observed between lifestyle or visual habits and PM. This may be related to the limited sample size or the characteristics of the case sources. Future studies are planned to include larger cohorts and further explore the potential role of lifestyle and visual behaviors in the development of PM.

Limitations of the Study

This study first constructs a diagnostic nomogram for pathological lesions in HM with TF based on interpretable clinical features and lifestyle habits. However, there are limitations. First, our study includes a limited sample, which may influence the interpretation of the findings. Second, since our validation set was internally generated by random sampling, more cases will need to be prospectively collected for external validation to evaluate the feasibility of the diagnostic model. Lastly, the generalizability of our findings may be limited, as the study population was drawn from a single geographic region. Therefore, multicenter and cross-regional studies are essential to enhance the generalizability and representativeness of our results.

Conclusion

In this study, an interpretable nomogram for predicting the risk of progression was developed and validated for PM in HM patients with TF. Among the independent predictors, axial length contributed the most to risk (12.5 points per 1 mm increase), followed by optic disc tilt ratio (5.63 points per 0.1 decrease), spherical equivalent (2.44 points per −1 D increase), education level (14.9 points for a bachelor's degree and 28.1 points for a master's degree compared with middle school), and extent of PPA >180° (10.8 points). This ranking provides an intuitive illustration of the relative importance of each risk factor. In the validation cohort, the model demonstrated an AUC of 0.827, with good sensitivity and specificity, confirming its clinical utility for early risk stratification at the HM stage. The findings offer clinicians a concise, reliable, and practical tool for identifying high-risk patients and guiding individualized follow-up strategies.

Data Sharing Statement

The original contributions presented in the study are included in the article. Further inquiries can be directed to the corresponding author.

Ethics Approval and Informed Consent

This study was conducted in accordance with the principles of the Declaration of Helsinki and was approved by the Institutional Review Board of The First Affiliated Hospital of Guangxi Medical University (Ethics Approval No.2023-K117-01). All participants or guardians of participants under 18 have signed the informed consent form.

Acknowledgments

Huiyi Zuo and Hai Huang should be considered as co-first authors for this study.

Author Contributions

All authors made a significant contribution to the work reported, whether that is in the conception, study design, execution, acquisition of data, analysis and interpretation, or in all these areas; took part in drafting, revising or critically reviewing the article; gave final approval of the version to be published; have agreed on the journal to which the article has been submitted; and agree to be accountable for all aspects of the work.

Funding

This work was supported by the Joint Project on Regional High-Incidence Diseases Research of Guangxi Natural Science Foundation under Grant (No. 2024GXNSFAA010322); Science and Technology Plan of Qingxiu District, Nanning City (No. 2020016); Medical and Health Appropriate Technology Development and Promotion Application Project of Guangxi Zhuang Autonomous Region (No. S2018093); Self-Funded Research Project of Health Commission of Guangxi Zhuang Autonomous Region (N0. Z20210589).

Disclosure

The authors declare that they have no competing interests in this work.

References

1. Holden BA, Fricke TR, Wilson DA, et al. Global prevalence of myopia and high myopia and temporal trends from 2000 through 2050. *Ophthalmology*. 2016;123:1036–1042. doi:10.1016/j.ophtha.2016.01.006
2. Flitcroft DI, He M, Jonas JB, et al. IMI - defining and classifying myopia: a proposed set of standards for clinical and epidemiologic studies. *Invest Ophthalmol Vis Sci*. 2019;60:M20–m30. doi:10.1167/iovs.18-25957
3. Landreneau JR, Hesemann NP, Cardonell MA. Review on the myopia pandemic: epidemiology, risk factors, and prevention. *Mo Med*. 2021;118:156–163.
4. Li Y, Foo LL, Wong CW, et al. Pathologic myopia: advances in imaging and the potential role of artificial intelligence. *Br J Ophthalmol*. 2023;107:600–606. doi:10.1136/bjophthalmol-2021-320926
5. Ohno-Matsui K, Kawasaki R, Jonas JB, et al. International photographic classification and grading system for myopic maculopathy. *Am J Ophthalmol*. 2015;159:877–883.e877. doi:10.1016/j.ajo.2015.01.022
6. Ruiz-Medrano J, Montero JA, Flores-Moreno I, et al. Myopic maculopathy: current status and proposal for a new classification and grading system (ATN). *Prog Retin Eye Res*. 2019;69:80–115. doi:10.1016/j.preteyeres.2018.10.005
7. Ohno-Matsui K, Lai TY, Lai CC, et al. Updates of pathologic myopia. *Prog Retin Eye Res*. 2016;52:156–187. doi:10.1016/j.preteyeres.2015.12.001
8. Ohno-Matsui K, Wu PC, Yamashiro K, et al. IMI Pathologic Myopia. *Invest Ophthalmol Vis Sci*. 2021;62:5. doi:10.1167/iovs.62.5.5
9. Yan YN, Wang YX, Yang Y, et al. Long-term progression and risk factors of fundus tessellation in the Beijing eye study. *Sci Rep*. 2018;8:10625. doi:10.1038/s41598-018-29009-1
10. Lyu H, Chen Q, Hu G, et al. Characteristics of fundal changes in fundus tessellation in young adults. *Front Med*. 2021;8:616249. doi:10.3389/fmed.2021.616249
11. Park HY, Lee K, Park CK. Optic disc torsion direction predicts the location of glaucomatous damage in normal-tension glaucoma patients with myopia. *Ophthalmology*. 2012;119:1844–1851. doi:10.1016/j.ophtha.2012.03.006
12. Chen Q, He J, Hu G, et al. Morphological characteristics and risk factors of myopic maculopathy in an older high myopia population-based on the new classification system (ATN). *Am J Ophthalmol*. 2019;208:356–366. doi:10.1016/j.ajo.2019.07.010
13. Sung MS, Kang YS, Heo H, et al. Characteristics of optic disc rotation in myopic eyes. *Ophthalmology*. 2016;123:400–407. doi:10.1016/j.ophtha.2015.10.018
14. Ye L, Chen Q, Hu G, et al. Distribution and association of visual impairment with myopic maculopathy across age groups among highly myopic eyes - based on the new classification system (ATN). *Acta Ophthalmol*. 2022;100:e957–e967. doi:10.1111/aos.15020
15. Prashar J, Tay N. Performance of artificial intelligence for the detection of pathological myopia from colour fundus images: a systematic review and meta-analysis. *Eye*. 2024;38:303–314. doi:10.1038/s41433-023-02680-z
16. Kim YC, Chang DJ, Park SJ, et al. Machine learning prediction of pathologic myopia using tomographic elevation of the posterior sclera. *Sci Rep*. 2021;11:6950. doi:10.1038/s41598-021-85699-0

17. Liu J, Wong DWK, Lim JH, et al. Detection of pathological myopia by PAMELA with texture-based features through an SVM approach. *J Healthc Eng*. 2010;1:657574. doi:10.1260/2040-2295.1.1.1
18. Tay E, Seah SK, Chan SP, et al. Optic disk ovality as an index of tilt and its relationship to myopia and perimetry. *Am J Ophthalmol*. 2005;139:247–252. doi:10.1016/j.ajo.2004.08.076
19. How AC, Tan GS, Chan YH, et al. Population prevalence of tilted and torted optic discs among an adult Chinese population in Singapore: the Tanjong Pagar Study. *Arch Ophthalmol*. 2009;127:894–899. doi:10.1001/archophthalmol.2009.134
20. Cohen SY, Dubois L, Nghiem-Buffet S, et al. Spectral domain optical coherence tomography analysis of macular changes in tilted disk syndrome. *Retina*. 2013;33:1338–1345. doi:10.1097/IAE.0b013e3182831364
21. Kim M, Choung HK, Lee KM, et al. Longitudinal changes of optic nerve head and peripapillary structure during childhood myopia progression on OCT: boramae myopia cohort study report 1. *Ophthalmology*. 2018;125:1215–1223. doi:10.1016/j.ophtha.2018.01.026
22. Koh V, Tan C, Tan PT, et al. Myopic maculopathy and optic disc changes in highly myopic young asian eyes and impact on visual acuity. *Am J Ophthalmol*. 2016;164:69–79. doi:10.1016/j.ajo.2016.01.005
23. Chen Q, He J, Yin Y, et al. Impact of the morphologic characteristics of optic disc on choroidal thickness in young myopic patients. *Invest Ophthalmol Vis Sci*. 2019;60:2958–2967. doi:10.1167/iovs.18-26393
24. Kim TW, Kim M, Weinreb RN, et al. Optic disc change with incipient myopia of childhood. *Ophthalmology*. 2012;119:21–26.e21–23. doi:10.1016/j.ophtha.2011.07.051
25. Wang YX, Panda-Jonas S, Jonas JB. Optic nerve head anatomy in myopia and glaucoma, including parapapillary zones alpha, beta, gamma and delta: histology and clinical features. *Prog Retin Eye Res*. 2021;83:100933. doi:10.1016/j.preteyeres.2020.100933
26. Fang Y, Yokoi T, Nagaoka N, et al. Progression of myopic maculopathy during 18-year follow-up. *Ophthalmology*. 2018;125:863–877. doi:10.1016/j.ophtha.2017.12.005
27. Yan YN, Wang YX, Yang Y, et al. Ten-year progression of myopic maculopathy: the beijing eye study 2001-2011. *Ophthalmology*. 2018;125:1253–1263. doi:10.1016/j.ophtha.2018.01.035
28. Biswas S, El Kareh A, Qureshi M, et al. The influence of the environment and lifestyle on myopia. *J Physiol Anthropol*. 2024;43:7. doi:10.1186/s40101-024-00354-7
29. Morgan IG, French AN, Ashby RS, et al. The epidemics of myopia: aetiology and prevention. *Prog Retin Eye Res*. 2018;62:134–149. doi:10.1016/j.preteyeres.2017.09.004
30. Wu PC, Huang HM, Yu HJ, et al. Epidemiology of myopia. *Asia Pac J Ophthalmol*. 2016;5:386–393. doi:10.1097/APO.0000000000000236
31. Gu SZ, Chang S. Pathologic Myopia. *Adv Exp Med Biol*. 2025;1467:281–283.
32. Baird PN, Saw SM, Lanca C, et al. Myopia. *Nat Rev Dis Primers*. 2020;6:99. doi:10.1038/s41572-020-00231-4
33. Tedja MS, Haarman AEG, Meester-Smoor MA, et al. IMI - myopia genetics report. *Invest Ophthalmol Vis Sci*. 2019;60:M89–m105. doi:10.1167/iovs.18-25965